J|A|C|S
ARTICLES
Published on Web 05/25/2006

Identification of a Quenching Species in Ruthenium Tris-Bipyridine Electroluminescent Devices

Leonard J. Soltzberg,*,† Jason D. Slinker,‡ Samuel Flores-Torres,§ Daniel A. Bernards,‡ George G. Malliaras,‡ Hector D. Abruña,§ Ji-Seon Kim,|| Richard H. Friend,|| Michael D. Kaplan,† and Velda Goldberg†

Contribution from the Departments of Chemistry and Physics, Simmons College, Boston, Massachusetts 02115, Department of Materials Science and Engineering, Cornell University, Ithaca, New York 14853-1501, Department of Chemistry and Chemical Biology, Cornell University, Ithaca, New York 14853-1301, and Cavendish Laboratory, Department of Physics, University of Cambridge, Cambridge CB3 0HE, United Kingdom

Received August 23, 2005; Revised Manuscript Received April 13, 2006; E-mail: lsoltzberg@simmons.edu

Abstract: We have used matrix-assisted laser desorption/ionization time-of-flight (MALDI-TOF) mass spectrometry and micro-Raman spectroscopy to identify a quenching species that is formed during operation of $[Ru(bpy)_3]^{2+}$ electroluminescent devices. We identify this performance-degrading product to be the oxo-bridged dimer $[(bpy)_2(H_2O)RuORu(OH_2)(bpy)_2]^{4+}$ and show this dimer to be an effective quencher of device luminescence. This work is the first to detect a specific chemical degradation product formed during iTMC OLED operation.

Introduction

The field of organic electronics has experienced dramatic advances in the past two decades, as devices like organic light emitting diodes (OLEDs) are now in commercial production.[1] A central issue in this field involves understanding the mechanisms of degradation of organic films under device operation conditions. To this extent, electroluminescent devices based on ionic transition metal complexes (iTMCs) such as $[Ru(bpy)_3]^{2+}$, where bpy is 2,2′-bipyridine,[2−7] represent a valuable system for degradation studies. These devices have recently attracted interest because, contrary to conventional OLEDs, they show efficient operation using air-stable electrodes.[2,7] This is due to the presence of mobile ions in the film that redistribute under bias and assist the injection of electrons and holes.[7,8] As a result, these devices allow one to probe the degradation of the organic film under conditions of bipolar injection, without interference from electrode degradation.

Even with air-stable electrodes, $[Ru(bpy)_3]^{2+}$ devices show an irreversible degradation that has been linked to the decay of the yield of photoluminescence of the $[Ru(bpy)_3]^{2+}$ film.[6,9] It was recently suggested that the formation of a quencher, such as $[Ru(bpy)_2(H_2O)_2]^{2+}$, could be the cause of $[Ru(bpy)_3]^{2+}$ device degradation.[9] However, this quenching species has not been found in a device to date. Identifying the chemical changes that take place during device operation may allow the synthesis of more stable materials and lead to significant improvements in device lifetime, not only in the case of iTMCs, but also for the general class of transition metal complex devices.[10]

We have used matrix assisted laser desorption/ionization time-of-flight (MALDI-TOF) mass spectrometry and micro-Raman spectroscopy to identify a quenching species that is formed during the operation of $[Ru(bpy)_3]^{2+}$ organic electroluminescent devices. We identify this performance-degrading product to be the oxo-bridged dimer $[(bpy)_2(H_2O)RuORu(OH_2)(bpy)_2]^{4+}$ and show this dimer to be an effective quencher of device luminescence. MALDI-TOF is capable of detecting femtomole quantities of analytes, and since ruthenium has several naturally occurring isotopes, mass spectra of ruthenium-containing species show distinctive patterns that are characteristic of the number of ruthenium atoms present.[11] Raman spectroscopy provides a complementary, noninvasive means of probing the makeup of the iTMC layer and confirms that the dimer is indeed generated by device operation. This work is the first to identify a specific chemical degradation product formed during the operation of an ionic transition metal complex (iTMC) device.

† Departments of Chemistry and Physics, Simmons College.
‡ Department of Materials Science and Engineering, Cornell University.
§ Department of Chemistry and Chemical Biology, Cornell University.
|| Cavendish Laboratory, Department of Physics, University of Cambridge.

(1) Malliaras, G. G.; Friend, R. H. *Physics Today* **2005**, *58*, 53.
(2) Slinker, J.; Bernards, D.; Houston, P. L.; Abruña, H. D.; Bernhard, S.; Malliaras, G. G. *Chem. Commun.* **2003**, *19*, 2392.
(3) Handy, E. S.; Pal, A. J.; Rubner, M. F. *J. Am. Chem. Soc.* **1999**, *121*, 3525.
(4) Gao, F. G.; Bard, A. J. *J. Am. Chem. Soc.* **2000**, *122*, 7426.
(5) Rudmann, H.; Shimida, S.; Rubner, M. F. *J. Am. Chem. Soc.* **2002**, *124*, 4918.
(6) Bernhard, S.; Barron, J. A.; Houston, P. L.; Abruña, H. D.; Ruglovksy, J. L.; Gao, X.; Malliaras, G. G. *J. Am. Chem. Soc.* **2002**, *124*, 13624.
(7) Gorodetsky, A. A.; Parker, S.; Slinker, J. D.; Bernards, D. A.; Wong, M. H.; Malliaras, G. G.; Flores-Torres, S.; Abruña, H. D. *Appl. Phys. Lett.* **2004**, *84*, 807.
(8) deMello, J. C. *Phys. Rev. B*, **2002**, *66*, 235210.
(9) Kalyuzhny, G.; Buda, M.; McNeill, J.; Barbara, P.; Bard, A. J. *J. Am. Chem. Soc.* **2003**, *125*, 6272.
(10) Holder, E.; Langeveld, B. M. W.; Schubert, U. S. *Adv. Mater.* **2005**, *17*, 1109.
(11) Ham, J. E.; Durham, B.; Scott, J. R. *J. Am. Soc. Mass Spectrom.* **2003**, *14*, 393.

Experimental Section

Solvents and reagents for synthesis were purchased from Aldrich and used without further purification. The details of the synthesis of $[Ru(bpy)_3]^{2+}(PF_6^-)_2$ have been described elsewhere.[6]

Synthesis of $[(bpy)_2(H_2O)RuORu(OH_2)(bpy)_2]^{4+}(PF_6^-)_4$. Dichlorobis(2,2′-bipyridyl)ruthenium(II), $Ru(bpy)_2Cl_2 \cdot 2H_2O$, was synthesized as previously described by Sullivan et al.[12]

$Ru(bpy)_2Cl_2 \cdot 2H_2O$ (500 mg, 1.03 mmol) was then dissolved in 30 mL of water, to which 175 mg of $AgNO_3$ was added, and heated to reflux with stirring for 2 days. Subsequently, 150 mL of water was added to the reaction flask, which was then filtered and the complex precipitated with 2.0 g of NH_4PF_6. The solution was filtered, washed with excess water, and dried with ether. A yield of 35% was obtained after recrystallization from a mixture of acetonitrile and ether. The material was subsequently characterized using cyclic voltammetry and UV−vis spectroscopy.

iTMC OLED Device Preparation. Devices for MALDI-TOF and Raman spectroscopy were spin-coated from acetonitrile solution and prepared with ITO and Au electrodes, as described previously.[6] Devices based on blends of $[Ru(bpy)_3]^{2+}(PF_6^-)_2$ and the oxo-bridged dimer were prepared similarly using acetone as the solvent.

Mass Spectrometry. Samples were prepared for MALDI-TOF mass spectrometry using the solvent-free method recently described by Trimpin et al.,[13] and elaborated by Hanton and Parees.[14] 10 mg of matrix (6-aza-2-thiothymine, nominal mass = 143 Da) was placed in a 4 mL cylindrical vial with two zinc plated BBs.[15] The solid analyte, scraped from the active area of the ITO/$[Ru(bpy)_3]^{2+}(PF_6^-)_2$/Au devices, and amounting to about 0.5 μg of material, was carefully transferred to the BBs using a sharpened microspatula, and the capped vial was agitated for 2 min on a vortex mixer. This process has been shown to produce an intimately mixed fine powder with a particle size of around 1 μm.[13] The powder was then pressed onto the stainless steel MALDI target and the excess blown away with a stream of air. This sample preparation method has several advantages of importance in the present work. There is no segregation of the analyte from the matrix as occurs upon solvent evaporation in the usual dried droplet preparation method. This characteristic results in excellent spot to spot reproducibility, which is important when there is limited analyte. Also, there is no question of solvent-mediated changes in the analyte. Because the sample is dry, the finely ground mixture can be kept intact and additional spectra can be run over a prolonged period of time.

Mass spectra were run on a Bruker Omniflex benchtop mass spectrometer in positive ion reflectron mode with a target potential of 19 kV, accelerating voltage of 14.8 kV, ion extraction delay of 300 ns, and laser power of around 160 μJ from a 337 nm nitrogen laser. This (relatively high) power was required to desorb/ionize the oxo-bridged dimer species. Spectra were recorded by averaging 50 laser shots. The instrument was calibrated using cesium iodide $Cs_{n+1}I_n^+$ positive clusters as an external reference.

Micro-Raman Spectroscopy. Raman spectra were obtained with a Renishaw 2000 Raman microscope. A HeNe laser (633 nm) excitation source was focused on the sample with either a 50× or a 100× microscope objective, and the scattered Raman signal was collected through the same objective and detected by a CCD camera. In the absence of electrical drive, no sign of degradation of the films upon exposure to the Raman laser was observed on the time scale of the measurements involved. All spectroscopic measurements were recorded in air. In the case of the devices, the spectra were recorded through the top (Au) electrode.

(12) Sullivan, B. P.; Salmon, D. J.; Meyer, T. J. *Inorg. Chem.* **1978**, *17*, 3334.
(13) Trimpin, S.; Rouhanipour, A.; Az, R.; Rader, H. J.; Müllen, K. *Rapid Commun. Mass Spectrom.* **2001**, *15*, 1365.
(14) Hanton, S. D.; Parees, D. M. *J. Am. Soc. Mass Spectrom.* **2005**, *16*, 90.
(15) Premium grade, 4.5 mm Zn plated, ultra smooth, steel air gun shot, Daisy Outdoor Products, Rogers, AR.

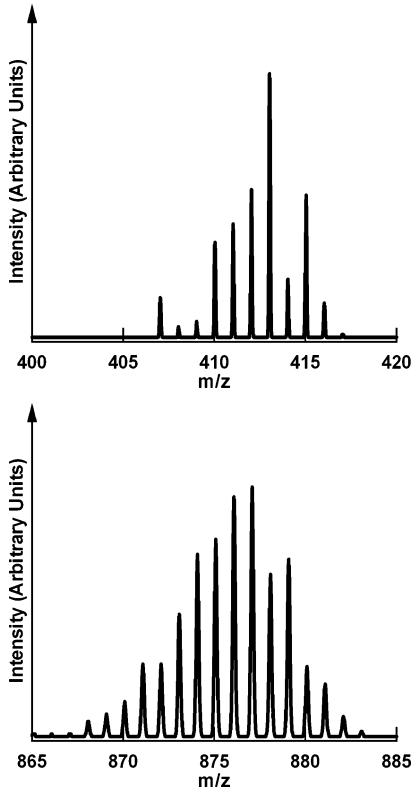

Figure 1. (Upper trace) Computed peak pattern for $[Ru(bpy)_2 - H]^+$ (one ruthenium atom). (Lower trace) Computed peak pattern for $[(bpy)_2(H_2O)RuORu(OH_2)(bpy)_2 - 3H]^+$ (two ruthenium atoms).

Thin film reference samples were prepared by spin-coating from solution onto 15 mm diameter Spectrosil substrates and baking for 2 h at 80 °C in a nitrogen glovebox. The Raman spectra for $[Ru(bpy)_3]^{2+}(PF_6^-)_2$ and $[(bpy)_2(H_2O)RuORu(OH_2)(bpy)_2]^{4+}$ reference samples were recorded immediately after removal from the glovebox. Otherwise, no special precaution was taken to prevent sample exposure to air.

The as-measured Raman spectra for $[Ru(bpy)_3]^{2+}(PF_6^-)_2$ and the virgin ITO/$[Ru(bpy)_3]^{2+}(PF_6^-)_2$/Au device are complicated by the presence of a fluorescence background which hampers observation of the intrinsic Raman shifts. For this reason, polynomial fits were applied to these spectra, and these fits were numerically subtracted from the as-measured spectra to provide the adjusted spectra presented in Figure 4. In this way, the relative scaling of the intrinsic Raman shifts is preserved.

Results and Discussion

Interpretation of Mass Spectra of Ruthenium-Containing Species. Ruthenium has six isotopes with natural abundances greater than 5%, which lead to characteristic patterns in the mass spectra of ruthenium-containing species and enable distinguishing mononuclear from dinuclear ruthenium compounds.

Computed peak patterns resulting from the naturally occurring isotopes of ruthenium are shown in Figure 1 for one- and two-ruthenium atom species. The patterns of relative intensity for the first four peaks in the sequence and also for the four peaks beginning with the highest peak are quite different in the one- and two-ruthenium cases. These patterns, in addition to the mass of a species (reported as the mass corresponding to the most abundant Ru isotope, 102 Da), make it possible to identify species from their mass spectra with confidence. This identification also depends on the fact that, in MALDI-TOF mass

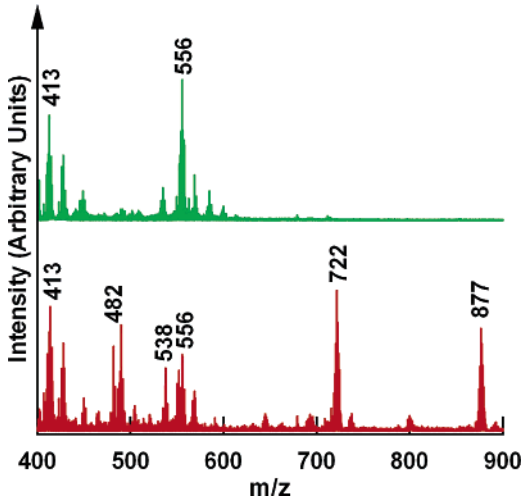

Figure 2. (Green upper trace) MALDI-TOF mass spectrum for material from a virgin ITO/$[Ru(bpy)_3]^{2+}(PF_6^-)_2$/Au device. (Red lower trace) MALDI-TOF mass spectrum for material from a ITO/$[Ru(bpy)_3]^{2+}(PF_6^-)_2$/Au device run for 2 h at 4 V dc.

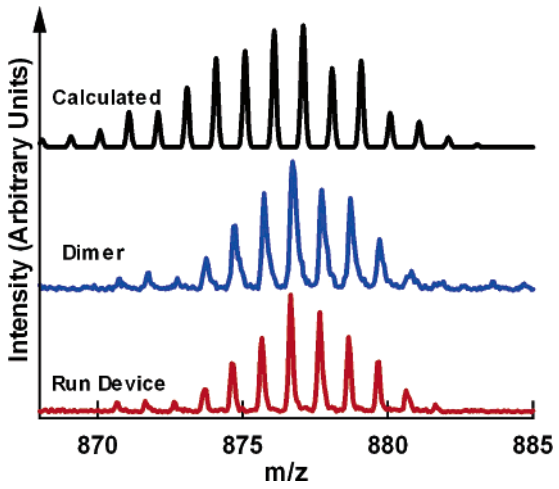

Figure 3. (Black upper trace) Calculated mass spectrum for $[(bpy)_2(H_2O)RuORu(OH_2)(bpy)_2 - 3H]^+$. (Blue middle trace) *m/z* 877 peak cluster for synthesized $[(bpy)_2(H_2O)RuORu(OH_2)(bpy)_2]^{4+}(PF_6^-)_4$. (Red lower trace) *m/z* 877 peak cluster for material from an ITO/$[Ru(bpy)_3]^{2+}(PF_6^-)_2$/Au device run for 2 h at 4 V dc.

spectrometry, the observed species are nearly always singly charged ions.[16]

Recent work has shown that care must be taken to avoid misinterpreting Ru isotope patterns if the peaks from a matrix adduct overlap those of the analyte species.[17] We have avoided that problem in the present work by using ATT as the matrix, which has a mass (143 Da), well separated from that of the bipyridyl ligands (156 Da).

Mass Spectra of Ruthenium-Containing Material from iTMC OLED Devices. Figure 2 shows the mass spectrum of material from a virgin ITO/$[Ru(bpy)_3]^{2+}(PF_6^-)_2$/Au device in the upper green trace. The principal peak clusters have one-ruthenium isotope patterns and correspond to $[Ru(bpy)_2 - H]^+$ (nominal mass for most abundant Ru isotope = 413)[11] and the matrix adduct $[Ru(bpy)_2 + ATT - H]^+$ (nominal mass for most abundant Ru isotope = 556). The predominance of these clusters

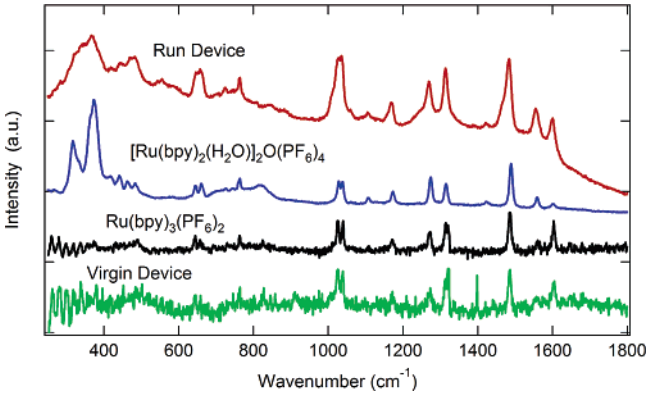

Figure 4. Raman spectra from a virgin ITO/$[Ru(bpy)_3]^{2+}(PF_6^-)_2$/Au device, known films of $[Ru(bpy)_3]^{2+}(PF_6^-)_2$ and $[(bpy)_2(H_2O)RuORu(OH_2)(bpy)_2]^{4+}(PF_6^-)_4$, and an ITO/$[Ru(bpy)_3]^{2+}(PF_6^-)_2$/Au device run to extinction. The spectra are offset along the *y*-axis for clarity.

and the absence of a $[Ru(bpy)_3 - H]^+$ cluster can be attributed to the high laser power used in this experiment.[11] Figure 2 also shows the mass spectrum of material from a ITO/$[Ru(bpy)_3]^{2+}(PF_6^-)_2$/Au device that was operated at 4V for 2 h (lower red trace). This device was on the same substrate as the virgin device and hence was subject to the identical processing and environmental exposure. Four significant dinuclear ruthenium peak clusters have appeared in the red trace, at *m/z* 877, 722, 538, and 482. The *m/z* 877 peak cluster corresponds to the calculated spectrum for $[(bpy)_2(H_2O)RuORu(OH_2)(bpy)_2 - 3H]^+$, while the *m/z* 722 cluster corresponds to $[(bpy)_2(H_2O)RuORu(OH_2)(bpy) - 2H]^+$. Because of interaction between the analyte and matrix in the MALDI "plume" produced by the laser pulse, analyte molecules can gain or lose varying numbers of hydrogen atoms; this phenomenon has been well documented for ruthenium complexes, for example.[18] The mass of the oxo-bridged dimer calculated for the most abundant ruthenium isotope is 880 Da, but that species has a charge of +4. Therefore, the corresponding +1 species observed in the MALDI mass spectrum is $[(bpy)_2(H_2O)RuORu(OH_2)(bpy)_2 - 3H]^+$ which appears at *m/z* 877.

The dinuclear clusters at *m/z* 538 and 482 are from related species containing fewer bpy ligands. It is unclear if these latter peaks are formed during device operation or via fragmentation of the *m/z* 877 species by the MALDI laser.

To elucidate the molecular identity of the 877 *m/z* peak cluster, Figure 3 presents a comparison of the calculated spectrum for $[(bpy)_2(H_2O)RuORu(OH_2)(bpy)_2 - 3H]^+$ (black trace) with the mass spectrum from a known synthetic sample of the dimer $[(bpy)_2(H_2O)RuORu(OH_2)(bpy)_2]^{4+}(PF_6^-)_4$ (blue trace). Figure 3 also shows the *m/z* 877 cluster from the device run at 4V (red trace), which is essentially identical to that of the synthesized dimer. This leads us to conclude that *the oxo-bridged dimer* $[(bpy)_2(H_2O)RuORu(OH_2)(bpy)_2]^{4+}$ *is being formed in ITO/*$[Ru(bpy)_3]^{2+}(PF_6^-)_2$*/Au devices during device operation.*

Various reaction pathways have been suggested concerning electrochemical formation of the oxo-bridged dimer from $[Ru(bpy)_3]^{2+}$.[19−23] The role and origin of water in this process remain an open question.

(16) Karas, M.; Glückmann, M.; Schäfer, J. *J. Mass Spectrom.* **2000**, *35*, 1.
(17) Soltzberg, L. J.; Do, K.; Lokhande, S.; Ochoa, S.; Tran, M. *Rapid Commun. Mass Spectrom.* **2005**, *19*, 2473.
(18) Ham, J. E.; Durham, B.; Scott, J. R. *J. Am. Soc. Mass Spectrom.* **2003**, *14*, 393, and references therein.
(19) Weaver, T. R.; Meyer, T. J.; Adeyemi, S. A.; Brown, G. M.; Eckberg, R. P.; Hatfield, W. E.; Johnson, E. C.; Murray, R. W.; Untereker, D. *J. Am. Chem. Soc.* **1975**, *97*, 3039.

Raman Spectroscopy of iTMC OLEDs. We have also confirmed the formation of oxo-bridged dimers in these devices using micro- Raman spectroscopy. Figure 4 compares the Raman spectra of a virgin ITO/$[Ru(bpy)_3]^{2+}(PF_6^-)_2$/Au device and a device driven for 2 h at 4V (the same operating conditions as described above) with the spectra from reference samples of $[Ru(bpy)_3]^{2+}(PF_6^-)_2$ and $[(bpy)_2(H_2O)RuORu(OH_2)(bpy)_2]^{4+}$. The spectrum of the virgin device shows the features of the $[Ru(bpy)_3]^{2+}(PF_6^-)_2$ reference sample. The Raman spectrum of the driven device differs noticeably from the virgin device. In particular, the driven device shows a pattern of peaks at around 380 cm^{-1} that are characteristic of the Ru−O−Ru moiety,[21,22] distinctive features that are also found in the $[(bpy)_2(H_2O)RuORu(OH_2)(bpy)_2]^{4+}$ reference sample. A time-resolved experiment has shown the incremental appearance of these peaks under electrical drive; this experiment will be reported elsewhere, as will additional details of the Raman work. These observations establish that dimerization indeed results from electrical drive, not from the MALDI laser.

Measurements on Dimer-Doped iTMC OLEDs. Table 1 gives the maximum luminance and external quantum efficiency of devices based on blends of $[Ru(bpy)_3]^{2+}(PF_6^-)_2$ and the dimer. Evidently, $[(bpy)_2(H_2O)RuORu(OH_2)(bpy)_2]^{4+}(PF_6^-)_4$ is an effective quencher of device luminescence, as the maximum luminance is reduced by over an order of magnitude relative to pristine for the 5 wt % devices. Additionally, the maximum external quantum efficiency is diminished by nearly 2 orders of magnitude over this range. These results suggest that this oxo-bridged dimer may significantly contribute to quenching of ITO/$[Ru(bpy)_3]^{2+}(PF_6^-)_2$/Au device luminescence.

Table 1. Maximum Luminance and External Quantum Efficiency of ITO/$[Ru(bpy)_3]^{2+}(PF_6^-)_2$/Au Devices with Various Concentrations of $[(bpy)_2(H_2O)RuORu(OH_2)(bpy)_2]^{4+}(PF_6^-)_4$, Average of 3 Devices

oxo-bridged dimer (wt %)	maximum luminance (cd/m^2)	maximum external quantum efficiency
0	1400 ± 100	1.07 ± 0.07%
0.1	1000 ± 100	0.97 ± 0.09%
1	560 ± 50	0.24 ± 0.04%
5	84 ± 7	0.015 ± 0.001%

Conclusions

We have used matrix-assisted laser desorption/ionization time-of-flight (MALDI−TOF) mass spectrometry to identify the oxo-bridged dimer $[(bpy)_2(H_2O)RuORu(OH_2)(bpy)_2]^{4+}$ unambiguously as a species that is formed in $[Ru(bpy)_3]^{2+}(PF_6^-)_2$ devices during device operation and have shown $[(bpy)_2(H_2O)RuORu(OH_2)(bpy)_2]^{4+}$ to be an effective quencher of device luminescence. Raman spectroscopy confirmed that the dimer is generated during the operation of the iTMC device.

Acknowledgment. Simmons College acknowledges support of the National Science Foundation (CHE-0216268 and DMR-0108497). The Cornell work was supported by the National Science Foundation (DMR-0094047), the Cornell Center for Materials Research (CCMR), and NYSTAR. J.D.S. was supported by a National Science Foundation Graduate Research Fellowship. D.A.B. was supported by a National Defense Science and Engineering Graduate Fellowship. We thank the reviewers for substantive comments and suggestions.

JA055782G

(20) Gilbert, J. A.; Eggleston, D. S.; Murphy, W. R., Jr.; Geselowitz, D. A.; Gersten, S. W.; Hodgson, D. J.; Meyer, T. J. *J. Am. Chem. Soc.* **1985**, *107*, 3855.
(21) Rotzinger, F. P.; Munavalli, S.; Comte, P.; Hurst, J. K.; Gratzel, M.; Pern., F.-J.; Frank, A. J. *J. Am. Chem. Soc.* **1987**, *109*, 6619.
(22) Schoonover, J. R.; Ni, J.; Roecker, L.; White, P. S.; Meyer, T. J. *Inorg. Chem.* **1996**, *35*, 5885.
(23) Fuller, Z. J.; Bare, W. D.; Kneas, K. A.; Xu, W.-Y.; Demas, J. N.; Degraff, B. A. *Anal. Chem.* **2003**, *75*, 2670.